Canadian Science Publishing | Canadian Geotechnical Journal

Thermo-mechanical behavior of a full-scale energy pile equipped with a spiral pipe configuration

Journal:	*Canadian Geotechnical Journal*
Manuscript ID	cgj-2020-0162.R2
Manuscript Type:	Article
Date Submitted by the Author:	22-Dec-2020
Complete List of Authors:	Wu, Di; Qingdao University of Technology Liu, Hanlong; Chongqing University Kong, Gangqiang; Hohai University Rotta Loria, Alessandro; Northwestern University
Keyword:	Energy pile, Spiral pipe, Thermo-mechanical behavior, Field test, Numerical simulation
Is the invited manuscript for consideration in a Special Issue? :	Not applicable (regular submission)

Thermo-mechanical behavior of a full-scale energy pile equipped with a spiral pipe configuration

Di Wu [1], Hanlong Liu [2], Gangqiang Kong [3,*], Alessandro F. Rotta Loria [4]

[1] School of Science, Qingdao University of Technology, Fushun Road No. 11, Qingdao, Shandong 266033, P.R. China. E-mail: wudi2009814@163.com.

[2] Key Laboratory of New Technology for Construction of Cities in Mountain Area, Shabei Road No.83, Chongqing University, Chongqing 400045, P.R. China. E-mail: wudi2009814@163.com. E-mail: cehliu@cqu.edu.cn.

[3] Key Laboratory of Ministry of Education for Geomechanics and Embankment Engineering, Hohai University, Xikang Road No.1, Nanjing, Jiangsu 210098, P.R. China; Key Laboratory of Geological Hazards on Three Gorges Reservoir Area of Ministry of Education, China Three Gorges University, Yichang, Hubei 443002, P.R. China. (Corresponding author) E-mail: gqkong1@163.com.

[4] Mechanics and Energy Laboratory, Department of Civil and Environmental Engineering, Northwestern University, Evanston, 2145 Sheridan Road, Illinois 60208, United States. E-mail: af-rottaloria@northwestern.edu.

Abstract

This study investigates the thermo-mechanical behavior of energy piles equipped with a spiral pipe configuration. The analysis is based on the results of a full-scale energy pile as well as 3-D thermo-mechanical finite element analyses. The thermo-mechanical behavior of two energy piles with five U-shaped pipes connected in series and parallel, characterized by the same total length of the piping network, is also analyzed numerically for comparison purposes. The results of this work highlight that energy piles equipped with a spiral pipe configuration are characterized by the lowest trends of average temperature variation and thermally induced vertical stress within their volume, as compared to energy piles equipped with five U-shaped pipe configurations connected in series or parallel. Considerable variations in temperature and thermally induced vertical stress arise in the vicinity of the piping network embedded in all of the considered energy piles. Nevertheless, energy piles equipped with a spiral pipe configuration appear the best solution for practical applications in comparison with U-shaped pipe configurations of the same total length, because they maximize the heat exchange that is achieved with the ground and minimize the associated thermally induced variations of their mechanical response.

Keywords: Energy pile; Spiral pipe; Thermo-mechanical behavior; Field test; Numerical simulation

Introduction

Ground source heat pump (GSHP) systems are widely used for the heating and cooling of structures and infrastructures because of their environmentally friendly character (Laloui and Rotta Loria 2019). Historically, geothermal boreholes have served as ground heat exchangers (GHEs) in GSHP systems. More recently, piles constituting the structural foundations of buildings have been increasingly used as GHEs to serve GSHP systems in the form of energy piles. In fact, by embedding within a pile shaft any configuration of pipes with a heat carrier fluid circulating into them, energy piles provide combined energy supply and structural support.

Over the past twenty years, an increasing number of studies have been performed to investigate the thermo-hydro-mechanical behavior of energy piles in an attempt to comprehensively address the energy, geotechnical and structural performance of such foundations. Various reviews on this subject are available (Bourne-Webb et al. 2016; Bourne-Webb and Freitas 2020; Fadejev et al. 2017; Loveridge et al. 2020). Examples of aspects governing the thermo-hydraulic behavior and the energy performance of energy piles include the conditions and properties of the ground (e.g., Ghasemi-Fare and Basu 2018), the geometry of the energy piles (e.g., Gao et al. 2008; Batini et al. 2015), the interference with the surface conditions (e.g., Bidarmaghz et al. 2016), as well as the significance and trend of thermal loads applied to such heat exchangers (e.g., Gawecka et al. 2017). Examples of features governing the thermo-mechanical behavior and the geotechnical and structural performance of energy piles include the restraint conditions (e.g., Goode and McCartney 2015; Zhou et al. 2018; Sutman et al. 2019; Wu et al. 2020), the significance and application sequence of mechanical and thermal loads (e.g., Laloui et al. 2003; Bourne-Webb et al. 2009; Rotta Loria et al. 2015), and the interaction between the piles (e.g., Salciarini et al. 2015; Rotta Loria and Laloui 2017a, b). In addition to the previous aspects, the pipe configuration installed in energy piles crucially characterizes their thermo-hydro-mechanical behavior and the related performance (e.g., Batini et al. 2015; Sani et al. 2019; Cecinato and Loveridge 2015).

Various investigations have addressed the thermo-hydro-mechanical behavior and the performance of energy piles equipped with single U-, double U- and W-shaped pipe configurations. Studies primarily focusing on the energy performance of such foundations have been achieved through full-scale experimental tests (e.g., Faizal et al. 2016; Gao et al. 2008), small-scale experimental tests (e.g., Kramer et al. 2015; Ghasemi-Fare and Basu 2018), numerical simulations (e.g., Gashti et al. 2014; Gao et al. 2008; Cecinato and Loveridge 2015) and analytical investigations (e.g., Zhang et al. 2013). Investigations primarily focusing on the geotechnical and structural performance of energy piles equipped with single U-, double U- and W-shaped pipe configurations have also been presented through full-scale experimental tests (e.g., Laloui et al. 2003; Bourne-Webb et al. 2009; Murphy et al. 2015), small-scale experimental tests (e.g., Wang et al. 2017), numerical simulations (e.g., Batini et al. 2015; Salciarini et al. 2015; Abdelaziz and Ozudogru 2016a) and analytical analyses (e.g., Rotta Loria and Laloui 2017b; Zhou et al. 2018).

In addition to the previous pipe configurations, the spiral-shaped arrangement is increasingly considered for energy piles, yielding to so-called spiral type energy piles. Investigations resorting to full-scale experimental tests (e.g., Zarrella et al. 2013; Yoon et al. 2015; Park et al. 2015), small-scale

experimental tests (e.g., Yang et al. 2016; Wang et al. 2017), numerical simulations (e.g., Bezyan et al. 2015; Zhao et al. 2017) and analytical analyses (e.g., Cui et al. 2011; Go et al. 2014; Xiang et al. 2015) have highlighted a remarkable energy performance of spiral type energy piles. Such a performance is typically more significant compared to that of energy piles equipped with single U-, double U- and W-shaped pipe configurations in comparable conditions. This is because of the typically greater total piping length per meter of energy pile on the ability of such heat exchangers to extract or inject thermal energy. Therefore, energy piles equipped with a spiral-shaped pipe configuration represent a particularly effective solution for the sake of geothermal energy exploitations, although the installation of the pipes along these foundations is less straightforward compared to other pipe configurations. Despite the available studies, scarce knowledge has been developed before this work about the geotechnical and structural performance of spiral type energy piles. As a consequence, the understanding of the influence of thermal loads (applied alone or in conjunction with mechanical loads) on the mechanical response of spiral type energy piles has been limited.

Looking at the previous challenge, this study presents an experimental and numerical investigation of the thermo-mechanical behavior of a spiral type energy pile to expand the knowledge about the geotechnical and structural performance of such foundations. The analysis is based on the results of a thermal response test performed on a full-scale spiral type energy pile as well as on 3-D finite element analyses. The study compares the obtained experimental and numerical results and investigates the temperature and thermally induced stress distributions caused within and along the tested energy pile by thermal loading. To expand this analysis, this paper further develops a comparison between the response of the investigated spiral type energy pile and another two energy piles, theoretically operating under the same conditions, with five U-shaped pipes connected in series and in parallel (involving the same total pipe length as the spiral pipe).

Field testing

Details of the test site

The full-scale field test presented in this study was carried out at Jiangyin city, China. A ground investigation was conducted before the construction of the energy pile. Four layers of stiff fine-grained soil were recognized along the energy pile depth. Noteworthy features and properties of these layers are reported in Table 1. The groundwater table level was found 0.5 m below the ground surface. The properties of the soil layers were determined through a series of laboratory tests on soil samples of each soil layer, including conventional physical parameters tests, oedometer tests, and thermal needle tests. The Young's modulus of the soil was assumed equal to 8.2 times of the modulus of compressibility determined by oedometer tests according to the empirical method proposed by Jia et al. (2008). The linear thermal expansion coefficient of the soil layers was not determined as a part of the experiments performed in this study. Di Donna and Laloui (2015) indicated that the linear thermal expansion coefficient of a heavily overconsolidated silty clay (OCR = 16) was $\alpha_T = 6\times10^{-6}$ $^{o}C^{-1}$. Abuel-Naga et al. (2007) and Liu et al. (2018) reported that the thermal expansion coefficient of fine-grained soils decreases with the OCR. Considering that the OCR at this site ranges between 5 and 5.5, a value of $\alpha_T = 1\times10^{-6}$ $^{o}C^{-1}$

was assumed to characterize all the soil layers (hypothesizing the correlation between α_T and OCR reported by Liu et al. (2018) to be valid for reducing the value of α_T reported by Di Donna and Laloui (2015) for OCR = 16 to a value for OCR = 5.25).

The schematic diagram of the spiral type energy pile is presented in Fig. 1. The energy pile was bored and made of reinforced concrete. The length and diameter of the pile are of L = 20 and D = 1 m, respectively. A reinforcing cage of 0.8 m in diameter was embedded in the pile shaft. A 190 m-long spiral-shaped polyethylene pipe was attached to the inner side of the reinforcing cage. The diameter D_s and pitches s of the pipe turns are 750 and 260 mm, respectively. The inner diameter and thickness of the pipe are 21 and 2 mm, respectively. The bottom of the spiral pipe was placed at 1 m above the energy pile toe to prevent potential pipe damage when pouring concrete. After the concrete of the pile shaft was cured, a 1.1-m-thick reinforced concrete slab connected to the head of the test pile was constructed. This slab connected the tested pile to the other four unheated piles in a row, which were located at a respective center-to-center spacing of 5.4 m. Further details about these piles are presented by Wu et al. (2020). No mechanical load was applied to the pile head at the time the test was conducted (before the construction of the superstructure). Ten vibrating wire strain gauges were installed along the test pile. Ten thermistors were also installed next to these strain gauges to measure the temperature variation in the pile shaft. Two thermistors were inserted into the inlet and outlet of the spiral pipe by using two caecal tubes (i.e., stainless-steel tubes with one end plugged) to monitor the temperature variation of circulating fluid.

Testing scheme

To assess the thermo-mechanical behavior of the spiral type energy pile, a thermal response test was performed. This test lasted a time of t = 240 hours and involved the application of a constant heating power of 4.8 kW. Such a thermal power was imposed through the circulation of a heat carrier fluid in the spiral-shaped pipe at a volumetric flow rate of 0.85 m^3/h (corresponding to a flow velocity of 0.72 m/s and a Reynolds number of Re = 18327 at a temperature of 30 ˚C) and was controlled using an electric heater. This significant flow rate was considered to decrease the testing time while being representative of fully turbulent conditions for the circulation of the heat carrier fluid in the pipes, which are preferable compared to laminar conditions for the sake of energy exploitations. Purified water was used as the heat carrier fluid. The temperature of the heat carrier fluid at the inlet and outlet of the pipe and the variations of temperature and strain along the energy pile were measured during the test.

Finite element modeling

Numerical modeling approach

Thermo-mechanical finite element analyses were conducted with the software COMSOL Multiphysics (COMSOL 2014) to get complementary information on the behavior and performance of the tested spiral type energy pile that may have been impossible to achieve otherwise. To serve the considered analyses, nine numerical models were built: three 3-D models of the spiral type energy pile with three linear thermal expansion coefficient of the soil layers, three 3-D models of an energy pile with five U-shaped pipes connected in series with three linear thermal expansion coefficient of the soil layers and three 3-D

models of an energy pile with five U-shaped pipes connected in parallel with three linear thermal expansion coefficient of the soil layers (Fig. 2).

The geometry of the 3-D model of the spiral type energy pile closely corresponds to the real conditions characterizing the field test (Fig. 2(a)). In this model, the tested spiral type energy pile and the four neighboring piles are simulated in the considered soil deposit, together with the beam connecting the head of such foundations. Linear entities are used to simulate the pipes. The spiral pipe, characterized by a total length of 190 m, is identical in the 3-D model and the field test (at least theoretically). The minimum distance in plan view of 10D from the external boundary of the model to the pile axis is considered to avoid boundary effects. A model depth of 2L is considered for the same aforementioned purpose.

The geometry of the 3-D models of the energy piles equipped with five U-shaped pipes connected in series and parallel is the same as the one characterizing the spiral type energy pile. Specifically, the pipe length is in all cases of 190 m (Fig. 2(b)), although the geometry of such a hydraulic circuit differs in different cases.

Assumptions and mathematical formulation

The following assumptions characterize the numerical simulations performed: (i) the displacements and deformations of all of the materials can be representatively described through a linear kinematic approach under quasi-static conditions (i.e., negligible inertial effects); (ii) the materials that constitute the energy pile foundation and soil are considered to be isotropic and are assumed to be purely conductive domains; (iii) the loads that are associated with this problem have a negligible impact on the variation of the hydraulic field in the soil; and (iv) all the materials are considered to be representatively described by a linear thermo-elastic behavior. In this study, 1-D pipe elements were used to model the fluid flow in the heat exchange pipes, and due account was made of turbulent flow conditions (COMSOL 2014). Based on the previous hypotheses, time-dependent, thermo-mechanical finite element analyses are carried out with the consideration of the circulation of the heat carrier fluid in the pipes. Previous numerical analyses employing the aforementioned mathematical approach have shown close agreement with experimental results (e.g., Rotta Loria and Laloui 2017a).

Boundary and initial conditions

The mechanical and thermal boundary conditions employed for the simulations performed in this study are presented in Fig. 2. Restrictions are applied to both the vertical and horizontal displacements on the base of the models (i.e., pinned boundary) and to the horizontal displacements on the sides (i.e., roller boundaries). No restrictions and mechanical loads are applied on top of the models, which reproduce the slab present at the head of the piles.

A constant temperature boundary condition is applied on top of the models and reproduces the ambient temperature that was recorded during the test. An adiabatic boundary condition characterizes all of the other external surfaces of the models.

To simulate the heat carrier fluid circulating in the pipes of the energy pile in the 3-D numerical models,

the experimentally recorded values of inlet temperature and velocity of the fluid are imposed throughout the simulations. The initial temperature considered for 3-D models is presented in Fig. 3. This variable temperature distribution with depth is applied to all of the modeled domains according to the profile measured experimentally just before the development of the test. The initial temperature gradually increases from 12 to 20 °C from the ground surface down to approximately z = 7 m of depth. Numerical extrapolation of this temperature suggests an approximately constant evolution with depth.

Tetrahedral and triangular elements characterize the 3-D models. Simulations are run in 60 steps, with results saved every 4 hours. The material properties of numerical models are presented in Table 1. Sensitivity analyses not presented herein show that a variation by ±17% in the assumed thermal expansion coefficient for the soil layers results in up to ±1.1% different variations in the stresses reported in this study.

Comparison between experimental and numerical results for the spiral type energy pile

Trends of temperature and thermally induced vertical stress

The temperature variations in correspondence with the top (i.e., z = 5.5 m), middle (i.e., z = 11.5 m) and bottom (i.e., z = 17.5 m) portions of the spiral type energy pile are presented in Fig. 4(a) by comparing the experimental data with the results of the 3-D numerical analyses. The temperature at the considered locations gradually increases over time due to the heating of the energy pile with constant thermal power. The temperature of the spiral type energy pile was about 34 °C at the end of the heating phase of the test. Different temperature trends characterize the three selected locations along the energy pile based on the results of the experimental tests and the 3-D numerical simulations. This result is due to the progressive heat exchange occurring in the pipe embedded in the energy pile, which induces a variation of both the heat carrier fluid and pile temperatures with depth.

Thermal loading of energy piles causes thermally induced stresses in such foundations because a portion of thermally induced pile deformation is restrained by the presence of the surrounding ground and the overlying superstructure. In the context of the analysis of experimental test results, thermally induced stresses can be calculated from the monitored thermally induced strains. Specifically, reference to one-dimensional and thermo-elastic conditions allows calculating the thermally induced vertical stress characterizing energy piles as follows (Laloui and Rotta Loria 2019):

$$\sigma_T = E(\varepsilon_T - \alpha_T \Delta T) \quad (1)$$

where E is the Young's modulus of the pile; ε_T is the observed vertical strain (calculated experimentally starting from the application of the thermal load to the energy pile and thus only accounting for a thermally induced contribution); α_T is the linear thermal expansion coefficient of the pile; and ΔT is the measured temperature variation. Thermally induced stresses derived in this way are compared with the obtained numerical results. The adopted sign convention assumes that compressive stresses are negative.

The trends of thermally induced vertical stress in correspondence with the top (i.e., z = 5.5 m), middle (i.e., z = 11.5 m) and bottom (i.e., z = 17.5 m) portions of the spiral type energy pile are presented in Fig. 4(b) by comparing the experimental data with the results of the 3-D numerical analyses. The heating of

the energy pile causes additional compressive vertical stresses along the pile shaft. The increase of compressive stress over time caused by thermal loading follows the temperature trend discussed in Fig. 4(a), with a reduced rate of variation over time. At the end of the test, experimentally determined values of thermally induced vertical stress of -1.66, -1.73 and -1.11 MPa characterize pile depths of z = 5.5, 11.5 and 17.5 m, respectively. Similar considerations can be highlighted with reference to the results obtained from the 3-D model, although a pronounced variation in thermally induced stress can be observed at the beginning of the test. The difference between the experimental and numerical results at the beginning of the test may be attributed to differences in the modeled and actual temperature distributions within and around the energy pile, as well as in the interplay between the thermally induced pile deformation and the restraint conditions.

The relationship between the thermally induced vertical stress and the associated temperature variation that characterize the spiral type energy pile at z = 5.5, 11.5 and 17.5 m is presented in Fig. 5 with reference to the experimental data and the results of the 3-D numerical analyses. Data obtained from EPFL test 2 to test 7 on an energy pile equipped with U-shaped pipes are plotted for reference (Amatya et al. 2012). Similar to previous evidence, an approximately linear increase in thermally induced vertical stress with temperature can be observed in the tested spiral type energy pile, although the considered pipe configurations are different. The observed variations of thermally induced vertical stress per unit temperature change vary with the location along the pile, although similar temperature variations characterize these locations (see Fig. 4(a)). This phenomenon can be associated with the different restraining influence of the soil layers surrounding the energy pile at different depths. In both the field test and numerical models, the largest thermally induced vertical stress is mobilized approximately at the mid-depth of the pile (i.e., z = 11.5 m), while the lowest thermally induced vertical stress is observed close to the toe of the energy pile as a consequence of the absence of the pipe in that location. Thermally induced vertical stress variations per unit temperature change in the spiral type energy pile range from -79 to -133 kPa/^{o}C, which are lower than the maximum thermally induced stress variations within the energy pile measured in EPFL tests 2 to 7, which was 153 kPa/°C (Amatya et al. 2012). This result is due to the fact that the thermally induced expansion of the investigated energy pile is markedly restrained by the presence of the slab only, while in the EPFL case both a slab and a stiff soil layer around the pile toe were present. The average degree of freedom along the pile tested in this study, defined as the ratio between the observed thermally induced strain and the strain under free thermal expansion conditions, ranges between DOF = 68 and 81% (at the end of the test), while the average values of this variable for EPFL tests 2 to 7 ranged between DOF = 47% and 60%, respectively (Laloui et al. 2003).

Variations of temperature and thermally induced vertical stress with depth

Fig. 6(a) presents a comparison between the temperature variation along the spiral type energy pile in correspondence with different longitudinal profiles at the end of the test using the experimental data and the results of the 3-D numerical analyses. An increase of temperature from the pile head to the toe can be observed. This phenomenon can be associated with the decrease of the heat carrier fluid temperature along the flow direction (from the bottom to the top of the spiral pipe) (Gao et al. 2008). A sudden

decrease in temperature at pile toe can be remarked because no pipes were installed in the bottom 1 m of the energy pile. The temperature profile predicted by the 3-D numerical analysis next to the spiral pipe shows remarkable fluctuations, with a maximum temperature difference with depth of about 2.5 °C. The considered changes decrease for an increase in the distance from the spiral pipe (e.g., toward the energy pile axis), leading to a smoother temperature profile along the pile. The observed temperature fluctuations in correspondence with the selected profile can be associated with the heat transfer associated with the spiral pipe. Similar observations were obtained in a previous investigation on a spiral type energy pile (Cui et al. 2011).

The thermally induced vertical stress along the spiral type energy pile in correspondence with different longitudinal profiles at the end of the test is presented in Fig. 6(b) using the experimental results and the data obtained from the 3-D numerical analyses. The maximum value of the thermally induced vertical stress is observed in correspondence with the middle portion of the spiral type energy pile. A considerable compressive vertical stress characterizes the head of the spiral type energy pile, which is associated with a significant head restraint played by the slab present at the ground surface. A relatively pronounced vertical stress is also observed at the pile toe and may be attributed to the stiffness of the end-bearing layer. These considerations agree with both the experimentally and theoretically informed schemes available in the literature to describe the thermo-mechanical behavior of energy piles (Bourne-Webb et al. 2013; Rotta Loria and Laloui 2018). Similar to the temperature profile next to the spiral pipe, the correspondent thermally induced vertical stress profile shows remarkable fluctuations. The considered fluctuations decrease for an increase in the distance from the pipe (e.g., toward the energy pile axis), leading to a smoother temperature profile along the pile, and highlight the coupling between the thermal and mechanical behavior of the energy pile. It should be noted that the heat transfer between the fluid, the pipes and the concrete constituting energy piles may be reproduced only approximately when 1-D pipe elements are used (Gawecka et al. 2020). This fact influences the interplay between the thermal and mechanical behaviors of energy piles. In this study, the coupling between the heat transfer taking place within the boundaires of the pipe and the surrounding concrete was achived by considering a heat source/sink in the global energy conservation equation to account for the contribution of the pipe (COMSOL 2014), providing consistent results with the experimental observations. This outcome may be considered representative of the accuracy of the numerical method employed.

Variations of temperature and thermally induced vertical stress with horizontal distance

The temperature along different horizontal lines crossing the spiral type energy pile axis at varying depths (i.e., L1-L5 corresponding to z = 11.86 m, 11.915 m, 11.98 m, 12.045 m and 12.11 m, respectively) across a single revolution of the coils is shown in Fig. 7(a) for the end of the test with reference to the results of the 3-D numerical analysis only. A relatively uniform temperature distribution characterizes the region of cut lines enclosed in the projection of the spiral pipe in the axial pile direction, except for some remarkable yet localized temperature variations (of about 2 °C) occurring at locations next to the pipe (see cut lines L1, L3 and L5). No abrupt temperature changes are highlighted for cut lines that do not cross the spiral pipe (see cut lines L2 and L4), presenting an almost symmetric temperature variation

with reference to the pile axis. The thermally induced vertical stress along different horizontal cut lines in the spiral type energy pile at the end of the test is shown in Fig. 7(b) with reference to the results of the 3-D numerical analysis. Similar to the temperature characterizing the cross-section of the spiral type energy pile, the thermally induced vertical stress more pronouncedly varies in correspondence with closer locations to the pipe compared to farther locations.

Thermally induced shear stress at the pile-soil interface

The thermally induced shear stress mobilized at the pile shaft of the spiral type energy pile at the end of the test is presented in Fig. 8 using the experimental results and the data obtained from the 3-D numerical analyses. The experimental mobilized shear stress is calculated from the difference in thermally induced axial stress within the energy pile at different depths as follows (Murphy et al. 2015):

$$f_{s,mob} = \frac{\Delta\sigma_T D}{4\Delta L} \tag{2}$$

where $\Delta\sigma_T$ is the difference in thermally induced axial stress determined by two adjacent strain gauges, and ΔL is the distance between strain gauges. The thermally induced shear stress determined through the 3-D numerical model represents an average of the shear stress mobilized along the circumference of the pile shaft. The adopted sign convention for the mobilized shear stress implies that positive shear stresses are associated with an upward pile displacement and negative shear stresses are associated with a downward pile displacement. Negative shear stress is mobilized in the upper portion of the spiral type energy pile shaft while positive shear stress is mobilized in the lower portion of the pile shaft during heating. Higher shear stress is mobilized near the pile toe compared to the pile head due to the presence of the head restraint. At 7.5 and 9.5 m depth, two reversals of the experimentally determined thermally induced shear stress were observed. These results can be attributed to the lower thermally induced vertical stress variations determined experimentally at these depths compared to those determined numerically (see Fig. 6(b)), which can be associated with (1) a lower restraint provided by the soil layer at these depths; (2) a farther location of the strain gauges from the pipes at these depths compared to the other strain gauges placed along the pile.

Comparison between the responses of energy piles equipped with spiral and U-shaped pipes

Inlet and outlet temperature trends of the heat carrier fluid

The trends of the inlet and outlet temperatures characterizing the heat carrier fluid circulating in the pipe of the three considered types of energy piles are presented in Fig. 9 by comparing the experimental data and the results of the 3-D numerical analyses. A relatively rapid increase of the inlet temperature is observed during the first 3 hours of the test (i.e., from 17 to 25 ^{o}C), with a less pronounced increase over time. The value of 38.8 ^{o}C is achieved in 240 hours from an initial temperature of 17 °C.

The experimental and numerical values of the outlet temperature of the spiral type energy pile are lower than the inlet fluid temperature according to the heating of the energy pile. A constant difference of 4.8 ^{o}C between the inlet and outlet fluid temperatures is observed after approximately 100 hours. The

values of outlet fluid temperature predicted by the 3-D numerical model of the spiral type energy pile are closely comparable with the experimental data.

A similar outlet temperature characterizes the spiral type energy pile and the energy pile with five U-shaped pipes connected in series, although the pipe configurations in these two piles are quite different. In contrast, a markedly different outlet temperature characterizes the energy pile with five U-shaped pipes connected in parallel. Specifically, a much greater outlet temperature (38 °C) is observed for the energy pile with the five U-shaped pipes connected in parallel as compared to the spiral type energy pile (34 °C) and the energy pile equipped with five U-shaped pipes connected in series (34 °C). The reason for this phenomenon is because a shorter pipe length from inlet to outlet characterizes the energy pile equipped with five U-shaped pipes in parallel. Therefore, the heat carrier fluid has less time to exchange heat with the (cooler) ground for the same inlet velocity and decrease in value.

The maximum temperature difference between the inlet and outlet of energy piles equipped with a spiral-shaped pipe and five U-shaped pipes connected in series is 4.8 °C, which is higher than the corresponding 0.8 °C of the energy pile with five U-shaped pipes connected in parallel. Based on this result, it might be considered that the heat exchange of energy piles equipped with a spiral-shaped pipe and five U-shaped pipes connected in series is more favourable than that associated with five U-shaped pipes connected in parallel. Not only the latter pipe configuration would yield a lower thermal power for the same inlet temperature and flow rate (negative from the standpoint of the lifecycle), but also a significantly greater number of pipes exiting the pile as compared to the other pipe configurations (negative from a construction perspective).

Temperature distributions in horizontal and vertical cross-sections of the energy pile

The temperature contours characterizing one vertical cross-section and one horizontal cross-section of energy piles equipped with a spiral pipe, five U-shaped pipes connected in series and five U-shaped pipes connected in parallel are presented in Fig. 10 with reference to the 3-D numerical results and the end of the reference heating phase. According to the observations presented in Fig. 7(a) for the spiral type energy pile, a more pronounced temperature variation can be observed for closer locations to the spiral pipe. This phenomenon can be highlighted from both the vertical (Fig. 10(a)) and horizontal (Fig. 10(b)) cross-sections. Considering the vertical cross-section, the average temperature within the region described by the projection of the pipe in the axial pile direction is 33.2 °C, while the maximum temperature is 36.2 °C, thus highlighting an 8.3% difference. Considering the horizontal cross-section, the average temperature within the region described by the projection of the pipe in the axial pile direction is 33.0 °C, while the maximum temperature is 35.8 °C, thus highlighting a 7.8% difference.

Similar to the considerations highlighted for the spiral type energy pile, a more pronounced temperature variation can be observed for closer locations to the pipes embedded in the two energy piles with U-shaped pipes connected in series and parallel. This phenomenon can be highlighted from both vertical (Fig. 10(c,e)) and horizontal (Fig. 10(d,f)) cross-sections. For example, considering the vertical cross-section of the energy pile equipped five U-shaped pipes connected in series, the average temperature within the region described by the projection of the pipe in the axial pile direction is 33.4 °C,

while the maximum temperature is 35.8 °C, thus highlighting a 6.7% difference. Considering the horizontal cross-section of this pile, the average temperature within the region described by the projection of the pipe in the axial pile direction is 33.2 °C, while the maximum temperature is 35.8 °C, thus highlighting a 7.3% difference. The corresponding numbers for the vertical and horizontal cross-sections selected for the energy pile equipped five U-shaped pipes connected in parallel are as follows: 35.1 °C, 37.0 °C, 5.1%, and 35.0 °C, 36.7 °C, 4.6%.

Based on these results, it can be appreciated that a more uniform temperature field characterizes the energy pile equipped with five U-shaped pipes connected in parallel for the same applied thermal power to the considered energy piles. Meanwhile, this is also the pile characterized by the most significant temperature level.

Thermally induced stress distributions in horizontal and vertical cross-sections of the energy pile

The contours of the thermally induced vertical stress characterizing one vertical cross-section and one horizontal cross-section of energy piles equipped with a spiral pipe, five U-shaped pipes connected in series and five U-shaped pipes connected in parallel are presented in Fig. 11 with reference to the 3-D numerical results and the end of the reference heating phase. According to the characteristics of the temperature field characterizing the considered energy piles that have been presented in Fig. 10, thermally induced stress concentrations can be observed next to the pipes.

Considering the vertical cross-section of the spiral type energy pile, the average thermally induced stress within the region described by the projection of the pipe in the axial pile direction is of -1.78 MPa, while the maximum thermally induced stress is of -3.29 MPa, thus highlighting a 45.9% difference. Considering the horizontal cross-section of the spiral type energy pile, the average thermally induced stress variation within the region described by the projection of the pipe in the axial pile direction is of -1.72 MPa while the maximum thermally induced stress is of -3.15 MPa, thus highlighting a 45.4% difference.

For two energy piles with five U-shaped pipes connected in series and parallel, stress concentrations for closer locations to the pipes can also be highlighted from both the vertical (Fig. 11(c,e)) and horizontal (Fig. 11(d,f)) cross-sections. Considering the vertical cross-section of the energy pile equipped five U-shaped pipes connected in series, the average thermally induced stress variation within the region described by the projection of the pipe in the axial pile direction is of -1.81 MPa, while the maximum thermally induced stress is of -3.13 MPa, thus highlighting a 42.1% difference. Considering the horizontal cross-section of this pile, the average thermally induced stress variation within the region described by the projection of the pipe in the axial pile direction is of -1.73 MPa while the maximum thermally induced stress is of -3.13 MPa, thus highlighting a 44.7% difference. The corresponding numbers for the vertical and horizontal cross-sections selected for the energy pile equipped five U-shaped pipes connected in parallel are as follows: -2.00 MPa, -3.07 MPa, 34.9%, and -1.95 MPa, -2.99 MPa, 34.8%.

Irrespective of the chosen pipe configuration, the aforementioned values of thermally induced vertical stresses should be considered in the performance-based design of energy piles at serviceability limit

states. More information about this subject has been reported by Rotta Loria et al. (2020). Complementary considerations about the role of creep in the design of energy piles, whose significance is tighly interconnected with stress level and stress fluctuations (e.g., thermally induced) within the constituting concrete, have been reported by Bourne-Webb (2020).

Trends of average temperature and thermally induced vertical stress

The trend of average temperature and average thermally induced vertical stress variations calculated over the entire volume of the energy piles in 3-D models are presented in Fig. 12(a) and Fig. 12(b), respectively. The energy pile equipped with five U-shaped pipes in parallel is the one characterized by the greatest average temperature variation and thermally induced stress. Lower temperature variations and thermally induced vertical stress variations are observed, in order, for the energy pile equipped with five U-shaped pipes in series and a spiral pipe. The maximum difference in the values of temperature and thermally induced vertical stress characterizing energy piles equipped with the spiral pipe and five U-shaped pipes in series is of less than 0.4 ^{o}C and 0.03 MPa, respectively. Due to the higher fluid temperature in each U-shaped pipe of the energy pile characterized by a parallel U-shaped pipe configuration, the maximum average temperature and thermally induced stress within this energy pile are about 1.9 ^{o}C and 0.16 MPa higher than those observed in the spiral type energy pile, respectively, for all of the three levels of soil linear thermal expansion coefficient.

The relationship between the average thermally induced vertical stress and the associated average temperature variation calculated over the entire volume of three modeled energy piles is presented in Fig. 12(c). The relationship between the considered variables is approximately the same and linear in all cases (i.e., 88 kPa/°C), irrespective of the fact that the pipe configurations of the modeled energy piles are different, significant local variations in temperature and thermally induced vertical stress can be observed next to the pipes of these energy piles, and different trends characterize pile temperature and thermally induced stress over time. This result is particularly significant for two reasons.

On the one hand, in accordance with the considerations of Caulk et al. (2016), the obtained result highlights that the average temperature variations characterizing energy piles, instead of the local and non-uniform temperature fluctuations that can be encountered within their cross-sections, govern their overall thermo-mechanical behavior. This result further suggests that the modeling of the global thermo-mechanical behavior of energy piles mostly depends on the restraint conditions and the material properties, making simplified analysis and design approaches that neglect specific pipe configurations appropriate, at least for preliminary estimates of the stresses involved. Localized temperature fluctuations, which can result in markedly non-uniform thermally induced stress distributions (also involving tensile stresses for piles subjected to heating thermal loads (Abdelaziz and Ozudogru 2016a) are indeed present. Appropriate selection of design temperature variations, through due account of the non-uniformity of the temperature field within energy piles (Abdelaziz and Ozudogru 2016b), is necessary for verification purposes of these and other energy geostructures (Rotta Loria 2019; Rotta Loria et al. 2020).

On the other hand, the obtained result suggests that there are indeed pipe configurations that are preferable than others. In fact, while the same relationship characterizes the temperature variation and

thermally induced vertical stress characterizing energy piles equipped with different pipe configurations, there are specific pipe configurations that maximize the heat exchange and minimize the associated thermally induced vertical stresses and are consequently preferable from a practical perspective. With reference to energy piles equipped with a spiral pipe or five U-shaped pipes connected in series or in parallel (involving the same total pipe length), the best solution appears to be the spiral type configuration. The reason for this is that, for the same total piping length and inlet velocity of the heat carrier fluid that circulates in the piping network, a spiral type configuration maximizes the heat exchange with the ground and minimizes the average thermally induced stress within energy piles. This statement appears to hold as long as pile diameters that can allow a relatively straightforward installation of spiral pipes are considered. Otherwise, pipes equipped with multiple U-shaped pipes connected in series could be a satisfactory alternative for satisfactory energy, geotechnical and structural performance of energy piles.

Conclusions

In this study, the thermo-mechanical behavior of a spiral type energy pile was investigated through a full-scale field test and 3-D finite element simulations. The thermo-mechanical behavior of two distinct energy piles with five U-shaped pipes connected in series and parallel (characterized by the same total length of the spiral pipe) was also analyzed for comparison purposes. Based on the results presented in this work, the following conclusions can be drawn:

1) Energy piles equipped with a spiral pipe configuration share the typical response observed to date upon thermal loading for energy piles with other pipe configurations (i.e. the most common pipe configuration of the energy pile used before is U-shaped), involving thermally induced expansive strains and compressive stresses upon heating as well as the mobilization of shear stresses at the pile-soil interface around the so-called null point.
2) Energy piles equipped with a spiral pipe configuration are characterized by the lowest trends of average temperature variation and thermally induced vertical stress within their volume, as compared to energy piles equipped with five U-shaped pipe configurations connected in series or parallel (with the same total pipe length). The highest trend of temperature variation and thermally induced vertical stress are observed for energy piles equipped with five U-shaped pipe configurations connected in parallel because of the lower temperature differential that characterizes the inlet and outlet of the individual pipes.
3) Although the trends of average temperature and average thermally induced stress variations vary for energy piles characterized by different pipe configurations, the relationship between these variables appears to be linear and indistinguishable as long as reversible conditions characterize the mechanics of the considered problem. That is, for a given average temperature variation, the overall mechanical response of energy piles predominantly depends on the restraint conditions and material properties of the considered problem rather than the pipe configuration. Nevertheless, there are indeed specific pipe configurations that maximize the heat exchange and minimize the associated thermally induced vertical stresses and are

consequently preferable from a practical perspective.

4) With reference to energy piles equipped with a spiral pipe or U-shaped pipes connected in series or in parallel (involving the same total pipe length), the best solution appears to be the spiral type configuration from energy, geotechnical and structural perspectives.

Acknowledgments

The work presented in this paper was supported by the National Natural Science Foundation of China (grant nos.51922037, 52008225). Hubei Key Laboratory of Disaster Prevention and Mitigation（China Three Gorges University）2020KJZ08.

References

Abdelaziz, S.L. and Ozudogru, T.Y. 2016a. Non-uniform thermal strains and stresses in energy piles. Environmental Geotechnics, 3(4):237-252. doi: 10.1680/jenge.15.00032

Abdelaziz, S.L. and Ozudogru, T.Y. 2016b. Selection of the design temperature change for energy piles. Applied Thermal Engineering, 107: 1036-1045. doi: 10.1016/j.applthermaleng.2016.07.067

Abuel-Naga, H.M., Bergado, D.T., Bouazza, A. 2007. Thermally induced volume change and excess pore water pressure of soft Bangkok clay. Engineering Geology 89: 144–154. doi: 10.1016/j.enggeo.2006.10.002

Amatya, B., Soga, K., Bourne-Webb, P.J., Amis, T., and Laloui, L. 2012. Thermo-mechanical behaviour of energy piles. Géotechnique, 62(6): 503–519. doi: 10.1680/geot.10.P.116

Batini, N., Rotta Loria, A.F., Conti, P., Testi, D., Grassi, W., and Laloui, L. 2015. Energy and geotechnical behaviour of energy piles for different design solutions. Applied Thermal Engineering, 86: 199-213. doi: 10.1016/j.applthermaleng.2015.04.050

Bezyan, B., Porkhial, S. and Mehrizi, A.A. 2015. 3-D simulation of heat transfer rate in geothermal pile-foundation heat exchangers with spiral pipe configuration. Applied Thermal Engineering, 87: 655-668. doi: 10.1016/j.applthermaleng.2015.05.051

Bidarmaghz, A., Narsilio, G.A., Johnston, I.W., and Colls, S. 2016. The importance of surface air temperature fluctuations on long-term performance of vertical ground heat exchangers. Geomechanics for Energy and the Environment, 6: 35-44. doi: 10.1016/j.gete.2016.02.003

Bourne-Webb, P. J. 2020. The role of concrete creep under sustained loading, during thermomechanical testing of energy piles. Computers and Geotechnics, 118: 103309. doi: 10.1016/j.compgeo.2019.103309

Bourne-Webb, P. J. and Freitas, T.M.B. 2020. Thermally-activated piles and pile groups under monotonic and cyclic thermal loading-A review. Renewable Energy, 147: 2572-2581. doi: 10.1016/j.renene.2018.11.025

Bourne-Webb, P., Burlon, S., Javed, S., Kürten, S. and Loveridge, F. 2016. Analysis and design methods for energy geostructures. Renewable and Sustainable Energy Reviews, 65: 402-419. doi: 10.1016/j.rser.2016.06.046

Bourne-Webb, P.J., Amatya, B. and Soga, K. 2013. A framework for understanding energy pile

behaviour. Proceedings of the Institution of Civil Engineers-Geotechnical Engineering, 166(2), 170-177. doi: 10.1680/geng.10.00098

Bourne-Webb, P.J., Amatya, B., Soga, K., Amis, T., Davidson, C., and Payne, P. 2009. Energy pile test at Lambeth College, London: geotechnical and thermodynamic aspects of pile response to heat cycles. Géotechnique, 59(3): 237-248. doi: 10.1680/geot.2009.59.3.237

Caulk, R., Ghazanfari, E. and Mccartney, J.S. 2016. Parameterization of a calibrated geothermal energy pile model. Geomechanics for Energy and the Environment, 5: 1-15. doi: 10.1016/j.gete.2015.11.001

Cecinato, F. and Loveridge, F.A. 2015. Influences on the thermal efficiency of energy piles. Energy, 82: 1021-1033. doi: 10.1016/j.energy.2015.02.001

COMSOL 2014. COMSOL Multiphysics Version 4.4: User's guide and reference manual. COMSOL, Burlington, Massachusetts, United States.

Cui, P., Li, X., Man, Y., and Fang, Z. 2011. Heat transfer analysis of pile geothermal heat exchangers with spiral coils. Applied Energy, 88(11): 4113-4119. doi: 10.1016/j.apenergy.2011.03.045

Di Donna, A. and Laloui L. 2015. Response of soil subjected to thermal cyclic loading: Experimental and constitutive study. Engineering Geology, 190: 65–76. doi: 10.1016/j.enggeo.2015.03.00

Fadejev, J., Simson, R., Kurnitski, J. et al. 2017. A review on energy piles design, sizing and modelling. Energy, 122: 390-407. doi: 10.1016/j.energy.2017.01.097

Faizal, M., Bouazza, A. and Singh, R.M. 2016. An experimental investigation of the influence of intermittent and continuous operating modes on the thermal behaviour of a full scale geothermal energy pile. Geomechanics for Energy and the Environment, 7(2): 80-101. doi: 10.1016/j.gete.2016.06.002

Gao, J., Zhang, X., Liu, J. et al. 2008. Numerical and experimental assessment of thermal performance of vertical energy piles: an application. Applied Energy, 85: 901-910. doi: 10.1016/j.apenergy.2008.02.010

Gashti, E.H.N., Uotinen, V.M. and Kujala, K. 2014. Numerical modelling of thermal regimes in steel energy pile foundations: a case study. Energy and Buildings, 69(3): 165-174. doi: 10.1016 /j.enbuild.2013.10.028

Gawecka, K.A., Taborda, D.M.G., and Potts, D.M., Cui, W., Zdravkovic, L., Kasri, M.S.H. 2017. Numerical modelling of thermo-active piles in London Clay. Proceedings of the Institution of Civil Engineers-Geotechnical Engineering, 170(3): 201-219. doi: 10.1680/jgeen.16.00096

Gawecka, K.A., Taborda, D.M.G., and Potts, D.M., Sailer, E., Cui, W.J., Zdravkovic, L. 2020. Finite-Element Modeling of Heat Transfer in Ground Source Energy Systems with Heat Exchanger Pipes. International Journal of Geomechanics, 20(5): 04020041. doi: 10.1061/(ASCE)GM.1943-5622.0001658

Ghasemi-Fare, O. and Basu, P. 2018. Influences of ground saturation and thermal boundary condition on energy harvesting using geothermal piles. Energy and Buildings, 165: 340-351. doi: 10.1016/ j.enbuild.2018.01.030

Go, G.H., Lee, S.R., Yoon, S., and Kang, H.B. 2014. Design of spiral coil PHC energy pile considering effective borehole thermal resistance and groundwater advection effects. Applied Energy, 125(2):

165-178. doi: 10.1016/j.apenergy.2014.03.059

Goode, J.C.I. and Mccartney, J.S. 2015. Centrifuge modeling of end-restraint effects in energy foundations. Journal of Geotechnical and Geoenvironmental Engineering, 141(8): 04015034. doi: 10.1061/(ASCE)GT.1943-5606. 0001333

Jia, D., Shi, F., Zheng, G. Xu, S., and An, L. 2008. Elastic modulus of soil used in numerical simulation of deep foundation pit. Chinese Journal of Geotechnical Engineering, S1: 155-158.

Kramer, C.A., Ghasemi-Fare, O. and Basu, P. 2015. Laboratory thermal performance tests on a model heat exchanger pile in sand. Geotechnical and Geological Engineering, 33(2): 253-271. doi: 10.1007/s10706 -014-9786-z

Laloui, L. and Rotta Loria, A.F. 2019. Analysis and design of energy geostructures: theoretical essentials and practical application. Academic Press.

Laloui, L., Moreni, M. and Vulliet, L. 2003. Comportement d'un pieu bi-fonction, fondation et échangeur de chaleur. Canadian Geotechnical Journal, 40(2): 388-402. doi: 10.1139/t02-117

Liu, H., Liu, H., Xiao, Y., and McCartney, J.S. 2018. Influence of Temperature on the Volume Change Behavior of Saturated Sand. Geotechnical Testing Journal, 41(4): 747-758. doi: 10.1520/GTJ20160308

Loveridge, F., McCartney, J.S., Narsilio, G.A., and Sanchez, M. 2020. Energy geostructures: A review of analysis approaches, in situ testing and model scale experiments. Geomechanics for Energy and the Environment, 22: 100173. doi: 10.1016/j.gete.2019.100173

Murphy, K.D., McCartney, J.S. and Henry, K.S. 2015. Evaluation of thermo-mechanical and thermal behavior of full-scale energy foundations. Acta Geotechnica, 10(2): 179-195. doi: 10.1007/s11440-013-0298-4

Park, S., Lee, D., Choi, H.J. et al. 2015. Relative constructability and thermal performance of cast-in-place concrete energy pile: coil-type GHEX (ground heat exchanger). Energy, 81: 56-66. doi: 10.1016/j.energy.2014.08.012

Rotta Loria, A.F. 2019. Performance-based design of energy pile foundations. The Journal of the Deep Foundations Institute, 12 (2): 94-107. doi: 10.1080/19375247.2018.1562600

Rotta Loria, A.F., Bocco, M., Garbellini, C., Muttoni, A., Laloui, L. 2020. The role of thermal loads in the performance-based design of energy piles. Geomechanics for Energy and the Environment, 21: 100153. doi: 10.1016/j.gete.2019.100153

Rotta Loria, A.F. and Laloui, L. 2017a. Thermally induced group effects among energy piles. Géotechnique, 67 (5): 374–393. doi: 10.1680/jgeot.16.P.039.

Rotta Loria, A.F. and Laloui, L. 2017b. Displacement interaction among energy piles bearing on stiff soil strata. Computers and Geotechnics, 90: 144-154. doi: 10.1016/j.compgeo.2017.06.008

Rotta Loria, A.F. and Laloui, L. 2018. Thermo-mechanical schemes for energy piles. International Symposium on Energy Geotechnics, SEG 2018, Lausanne, Switzerland, pp: 218-225.

Rotta Loria, A.F., Gunawan, A. and Shi, C., Laloui, L., and Ng, C.W.W. 2015. Numerical modelling of energy piles in saturated sand subjected to thermo-mechanical loads. Geomechanics for Energy and the Environment, 1: 1-15. doi: 10.1016/j.gete.2015.03.002

Salciarini, D., Ronchi, F., Cattoni, E., and Tamagnini, C. 2015. Thermomechanical effects induced by energy piles operation in a small piled raft. International Journal of Geomechanics, 15(2): 04014042. doi: 10. 1061/(ASCE)GM.1943-5622.0000375

Sani, A.K., Singh, R.M., Tsuha, C.H.C., and Cavarretta, I. 2019. Pipe–pipe thermal interaction in a geothermal energy pile. Geothermics, 81: 209-223. doi: 10.1016/j.geothermics.2019.05.004

Sutman, M., Brettmann, T. and Olgun, C.G. 2019. Full-scale in-situ tests on energy piles: Head and base-restraining effects on the structural behaviour of three energy piles. Geomechanics for Energy and the Environment, 18: 56–68. doi: 10.1016/j.gete.2018.08.002

Wang, C., Liu, H., Kong, G., and Ng, C.W.W. 2017. Different types of energy piles with heating-cooling cycles. Proceedings of the Institution of Civil Engineers-Geotechnical Engineering, 170(3): 220-231. doi: 10.1680/ jgeen.16.00061

Wu, D., Liu, H., Kong, G., and Ng, C.W.W. 2020. Interactions of an energy pile with several traditional piles in a row. Journal of Geotechnical and Geoenvironmental Engineering, 146(4): 06020002. doi: 10.1061/(ASCE)GT.1943- 5606.0002224

Xiang, Y., Su, H., Gou, W., Zhao, Y., Kuang, W., Liu, Z. et al. 2015. A new practical numerical model for the energy pile with spiral coils. International Journal of Heat and Mass Transfer, 91: 777-784. doi: 10.1016/j.ijheatmasstransfer.2015.08.028

Yang, W., Lu, P. and Chen, Y. 2016. Laboratory investigations of the thermal performance of an energy pile with spiral coil ground heat exchanger. Energy and Buildings, 128: 491-502. doi: 10.1016/j.enbuild.2016.07.012

Yoon, S., Lee, S.R., Go, G.H., and Park, S. 2015. An experimental and numerical approach to derive ground thermal conductivity in spiral coil type ground heat exchanger. Journal of the Energy Institute, 88(3): 229-240. doi: 10.1016/j.joei.2014.10.002

Zarrella, A., Carli, M.D. and Galgaro, A. 2013. Thermal performance of two types of energy foundation pile: helical pipe and triple U-tube. Applied Thermal Engineering, 61(2): 301-310. doi: 10.1016/j.appl thermaleng.2013.08.011

Zhang, W., Yang, H., Lu, L., and Fang, Z. 2013. The analysis on solid cylindrical heat source model of foundation pile ground heat exchangers with groundwater flow. Energy, 55(1): 417-425. doi: 10.1016/j.energy.2013.03.092

Zhao Q., Liu F., Liu C., Tian, M., and Chen, B. 2017. Influence of spiral pitch on the thermal behaviors of energy piles with spiral-tube heat exchanger. Applied Thermal Engineering, 125: 1280-1290. doi: 10.1016/j.applthermaleng.2017.07.099

Zhou, H., Kong, G., Liu, H., and Laloui, L. 2018. Similarity solution for cavity expansion in thermoplastic soil. International Journal for Numerical and Analytical Methods in Geomechanics, 42(2): 274- 294. doi: 10.1002/nag. 2724

Table 1 Soil, energy pile and pipe material parameters

Material	Soil type	Depth (m)	ρ (g/cm^3)	λ (W/(m.K))	c_p (J/(kg.K))	E (MPa)	v (-)	α_T ($\times 10^{-6}$ °C^{-1})	S_r (%)	I_p (-)
Soil										
Layer 1	Silty clay	0~6.2	1.88	1.66	2900	120	0.3	1	93.3	10.3
Layer 2	Gravel clay	6.2~10.3	2.03	1.76	2600	100	0.32	1	98.5	13.3
Layer 3	Silty clay	10.3~19.1	2.02	1.85	2500	130	0.3	1	97.6	11.5
Layer 4	Sandy clay	Below 19.1	2.07	1.85	2500	200	0.25	1	100	8.6
Concrete	—	—	2.50	1.90	1000	40000	0.2	10	—	—
Pipe	—	—	—	0.46	—	—	—	—	—	—

Notes: γ is the unit weight, λ is the thermal conductivity, c_p is the specific heat, E is the Young's modulus, v is the Poisson's ratio, and α_T is the linear thermal expansion coefficient, S_r is the saturation, I_p is the plasticity index.

Figure Captions:

Fig. 1. Schematic diagram of the energy pile: (a) vertical cross-section of the spiral type energy pile; (b) plan view of the spiral type energy pile; (c) plan view of the energy pile with five U-shaped pipes in series; and (d) plan view of the energy pile with five U-shaped pipes in parallel.

Fig. 2. Details of the numerical models: (a) mesh and boundary conditions of the 3-D models; and (b) geometry of the three types of heat exchanger pipes.

Fig. 3. Initial ground temperature distribution.

Fig. 4. Trends of (a) temperature and (b) thermally induced stress within the spiral type energy pile at different depths.

Fig. 5. Variations of thermally induced vertical stress of the spiral type energy pile for a given (localized) pile temperature increment.

Fig. 6. Profiles of (a) temperature and (b) thermally induced stress along the spiral type energy pile at the end of the test for different positions within the pile.

Fig. 7. Variations of (a) temperature and (b) thermally induced stress along different horizontal cut lines in the spiral type energy pile at the end of the numerical simulations.

Fig. 8. Profiles of thermally induced shear stress at the pile-soil interface for the end of the test.

Fig. 9. Inlet and outlet temperature trends of the heat carrier fluid circulating in the pipe of the energy pile.

Fig. 10. Temperature contours within energy piles equipped with a spiral pipe configuration, five U-shaped pipes connected in series and five U-shaped pipes connected in parallel at the end of the reference heating period: (a) elevation and (b) plan views of the spiral type energy pile; (c) elevation and (d) plan view of the energy pile with five U-shaped pipes in series. (e) elevation and (f) plan views of the energy pile with five U-shaped pipes in parallel.

Fig. 11. Thermally induced vertical stress contours within energy piles equipped with a spiral pipe configuration, five U-shaped pipes connected in series and five U-shaped pipes connected in parallel at the end of the reference heating period: (a) elevation and (b) plan views of the spiral type energy pile; (c) elevation and (d) plan view of the energy pile with five U-shaped pipes in series. (e) elevation and (f) plan views of the energy pile with five U-shaped pipes in parallel.

Fig. 12. Comparison between the average response of energy piles equipped with a spiral pipe configuration, five U-shaped pipes connected in series and five U-shaped pipes connected in parallel at the end of the numerical simulations: (a) average pile temperature trend; (b) average thermally induced vertical stress trend; and (c) relationship between the average thermally induced vertical stress and the associated average temperature variation.

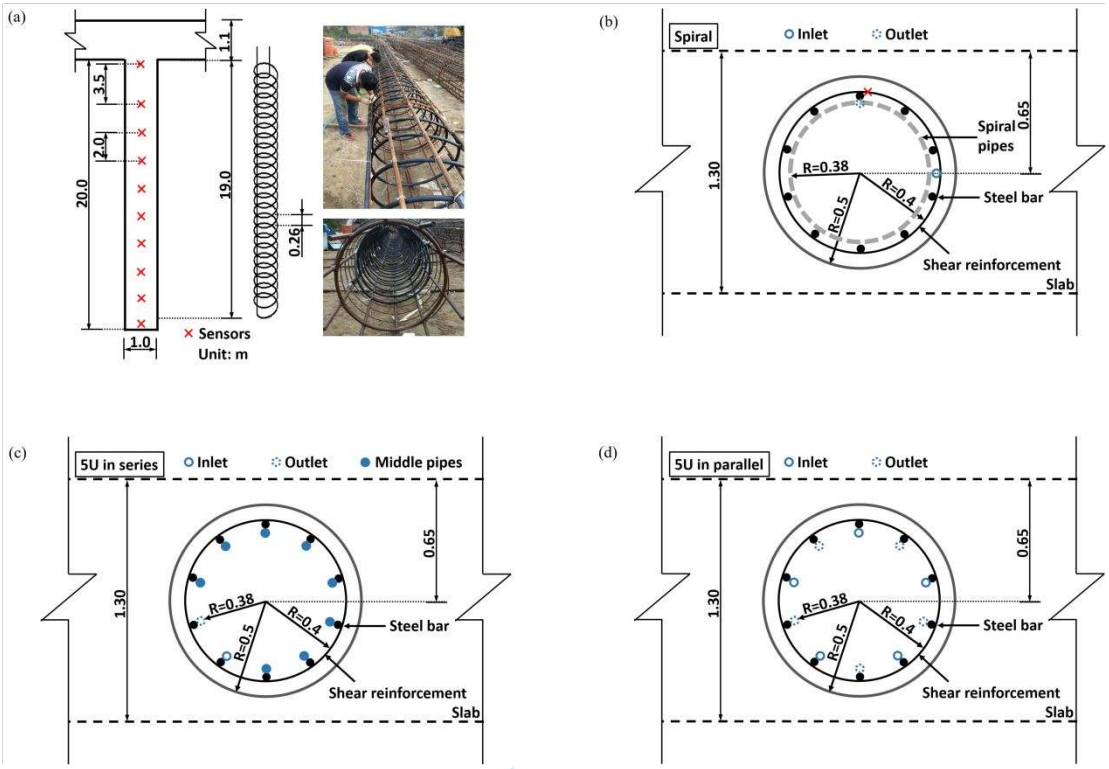

Fig. 1. Schematic diagram of the energy pile: (a) vertical cross-section of the spiral type energy pile; (b) plan view of the spiral type energy pile; (c) plan view of the energy pile with five U-shaped pipes in series; and (d) plan view of the energy pile with five U-shaped pipes in parallel.

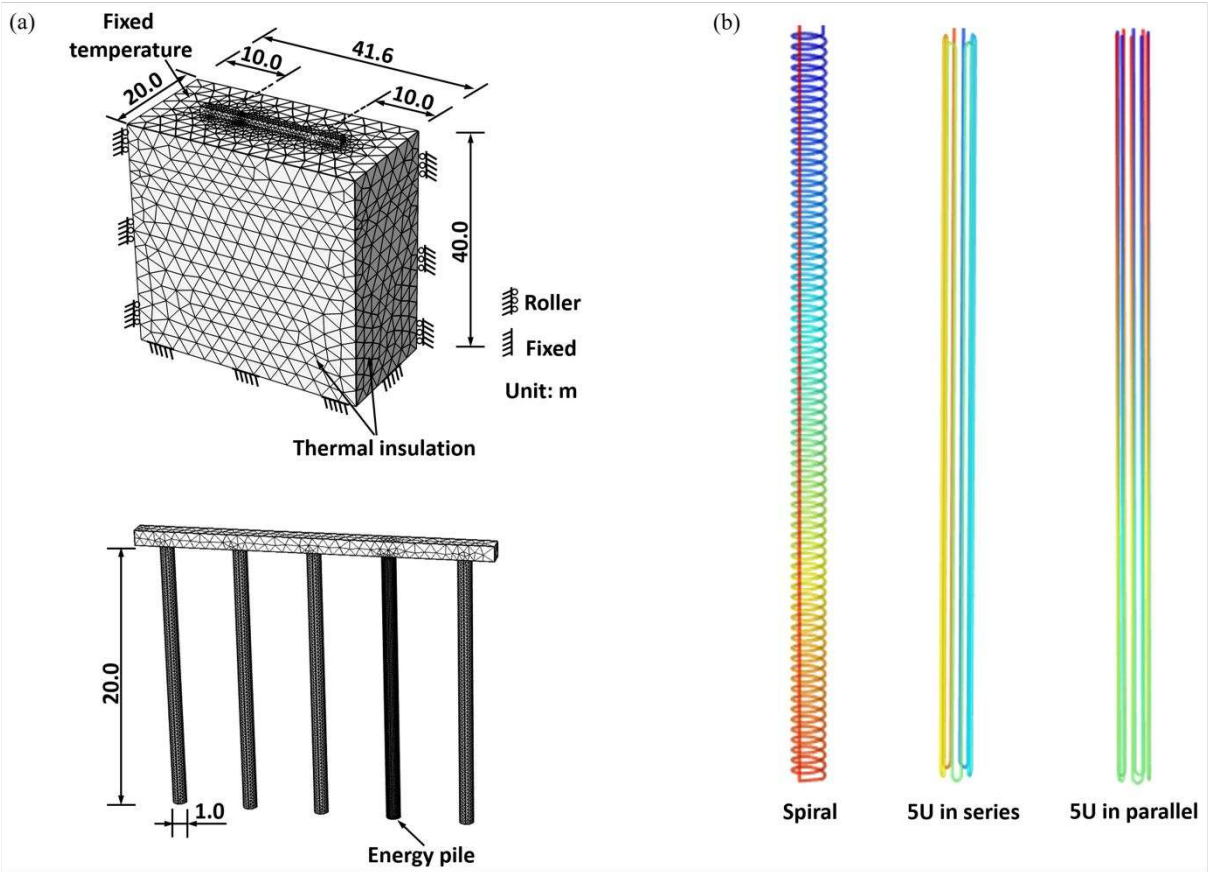

Fig. 2. Details of the numerical models: (a) mesh and boundary conditions of the 3-D models; and (b) geometry of the three types of heat exchanger pipes.

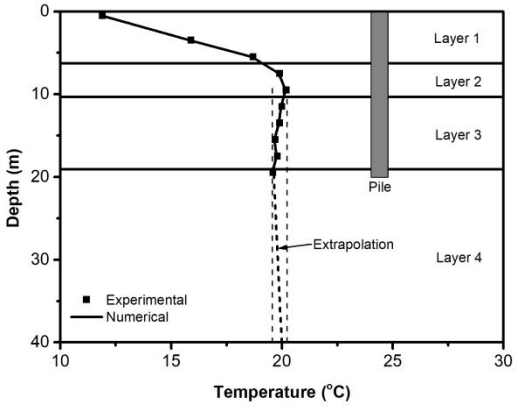

Fig. 3. Initial ground temperature distribution.

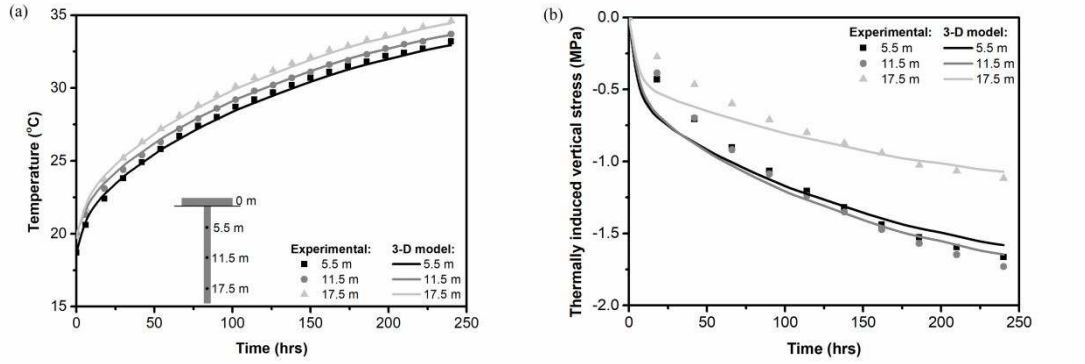

Fig. 4. Trends of (a) temperature and (b) thermally induced stress within the spiral type energy pile at different depths.

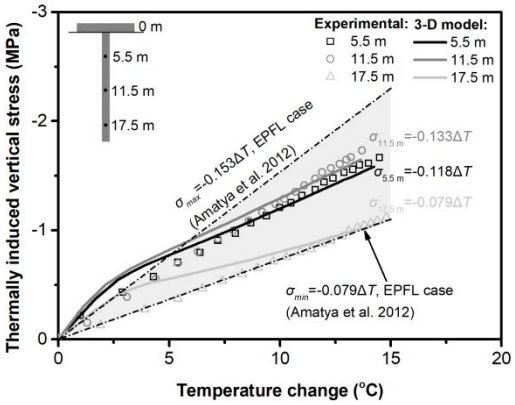

Fig. 5. Variations of thermally induced vertical stress of the spiral type energy pile for a given (localized) pile temperature increment.

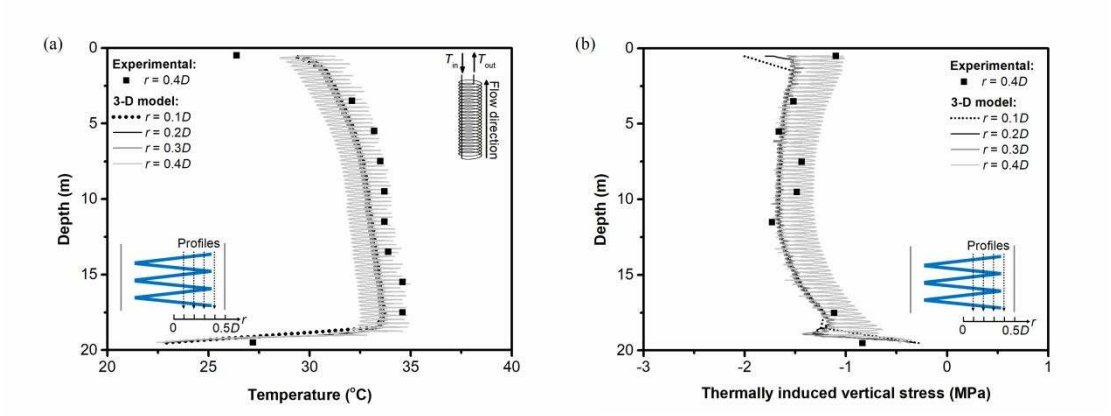

Fig. 6. Profiles of (a) temperature and (b) thermally induced stress along the spiral type energy pile at the end of the test for different positions within the pile.

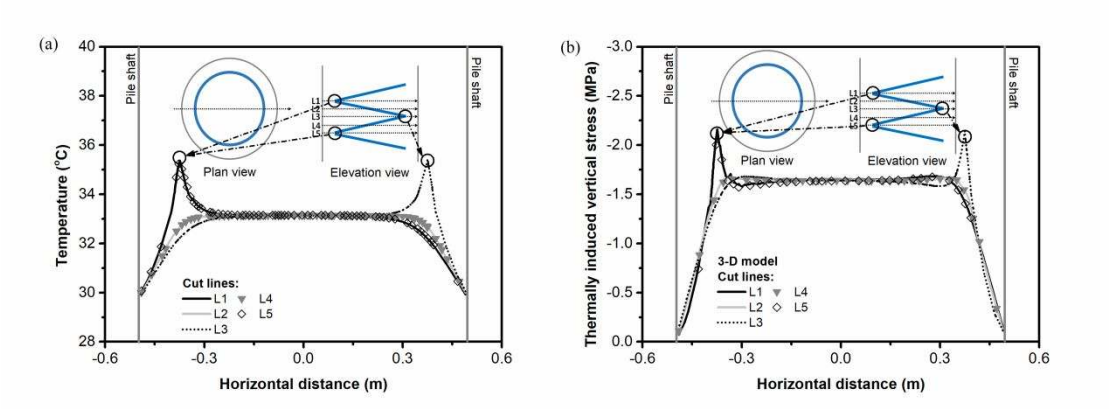

Fig. 7. Variations of (a) temperature and (b) thermally induced stress along different horizontal cut lines in the spiral type energy pile at the end of the numerical simulations.

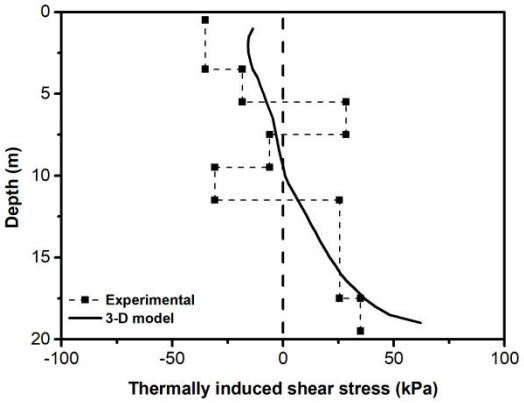

Fig. 8. Profiles of thermally induced shear stress at the pile-soil interface for the end of the test.

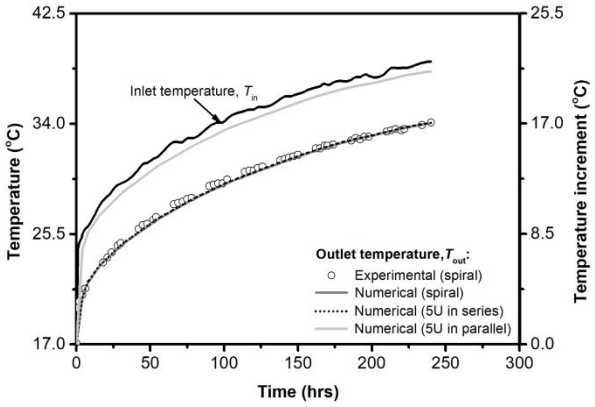

Fig. 9. Inlet and outlet temperature trends of the heat carrier fluid circulating in the pipe of the energy pile.

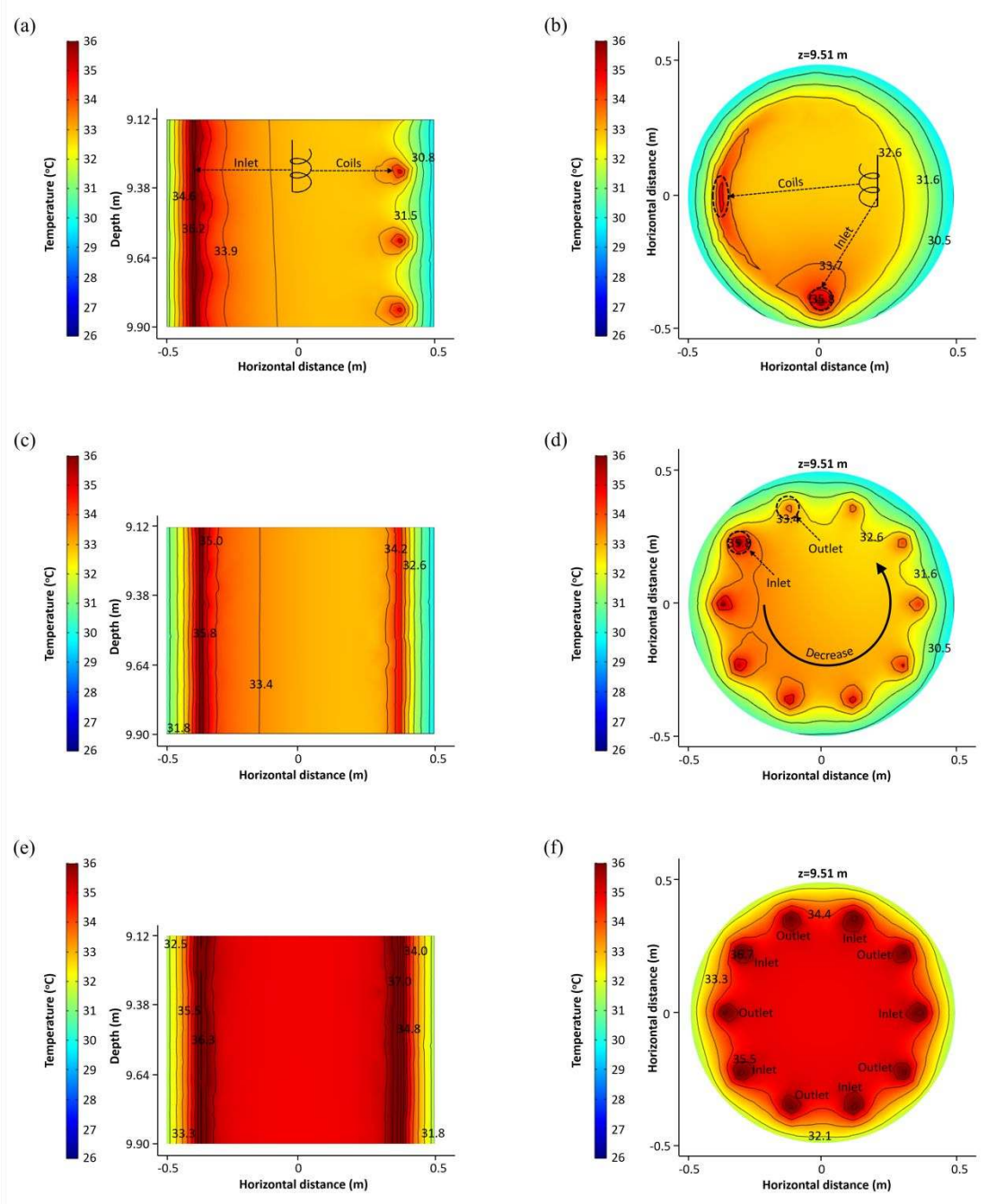

Fig. 10. Temperature contours within energy piles equipped with a spiral pipe configuration, five U-shaped pipes connected in series and five U-shaped pipes connected in parallel at the end of the reference heating period: (a) elevation and (b) plan views of the spiral type energy pile; (c) elevation and (d) plan view of the energy pile with five U-shaped pipes in series. (e) elevation and (f) plan views of the energy pile with five U-shaped pipes in parallel.

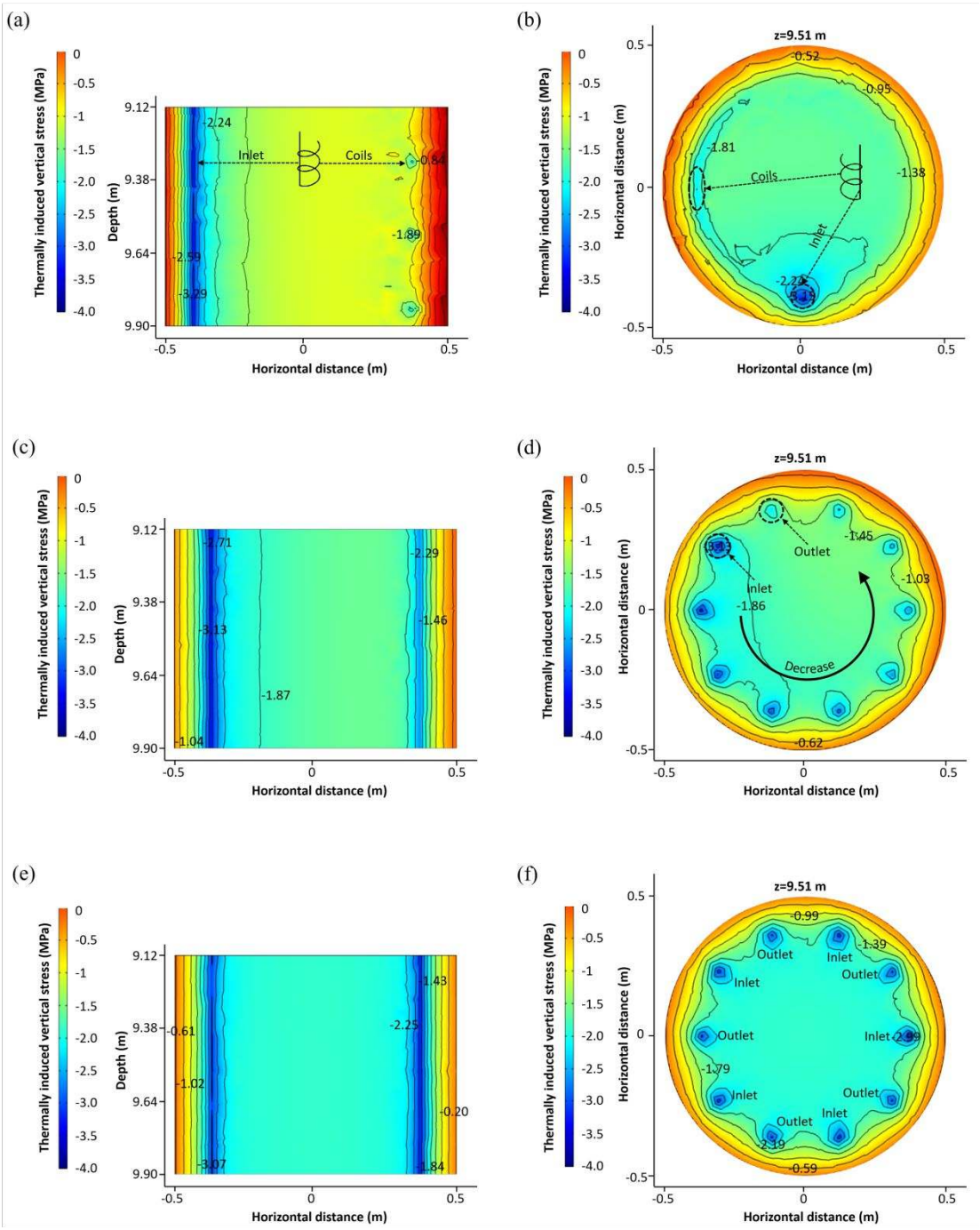

Fig. 11. Thermally induced vertical stress contours within energy piles equipped with a spiral pipe configuration, five U-shaped pipes connected in series and five U-shaped pipes connected in parallel at the end of the reference heating period: (a) elevation and (b) plan views of the spiral type energy pile; (c) elevation and (d) plan view of the energy pile with five U-shaped pipes in series. (e) elevation and (f) plan views of the energy pile with five U-shaped pipes in parallel.

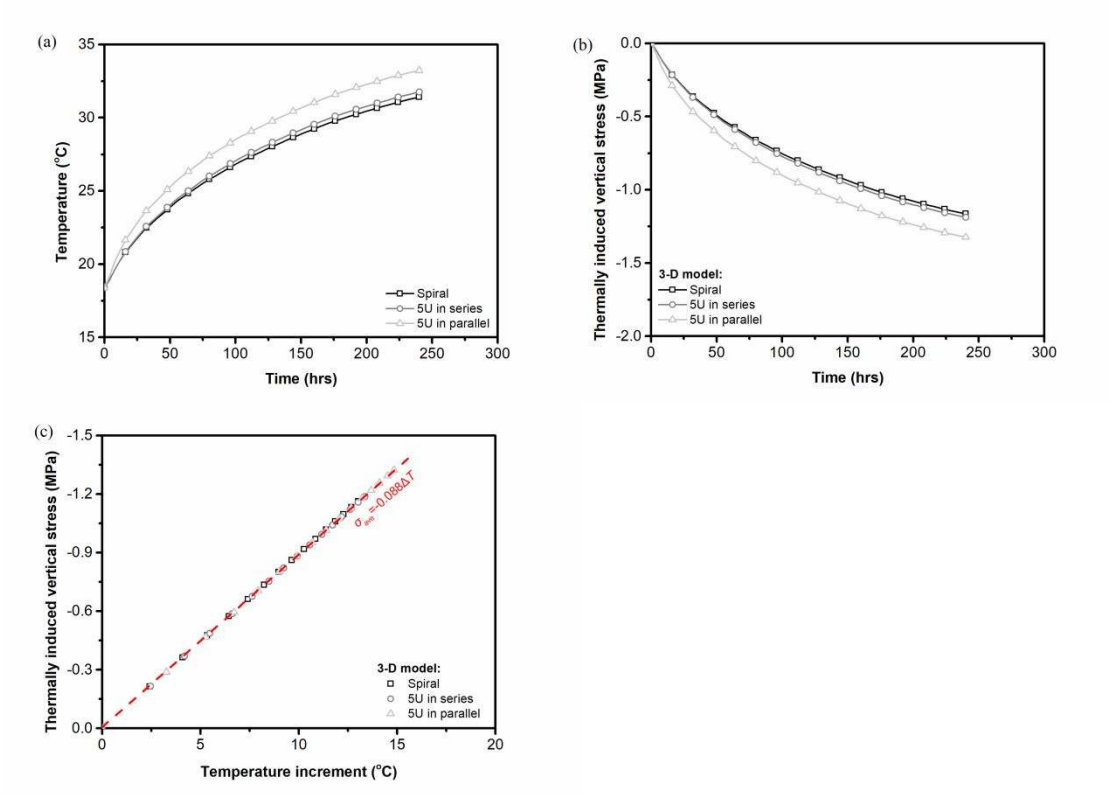

Fig. 12. Comparison between the average response of energy piles equipped with a spiral pipe configuration, five U-shaped pipes connected in series and five U-shaped pipes connected in parallel at the end of the numerical simulations: (a) average pile temperature trend; (b) average thermally induced vertical stress trend; and (c) relationship between the average thermally induced vertical stress and the associated average temperature variation.